Evidence for Electron-Hole Pair Excitation in the Associative Desorption of H_2 and D_2 from Au(111)

Supporting Information

Quan Shuai,[†,‖] Sven Kaufmann,*[†,‡] Daniel J. Auerbach,[†,‡] Dirk Schwarzer,[†,‡] and Alec M. Wodtke[†,‡,§]*

[†]Department of Dynamics at Surfaces, Max Planck Institute for Biophysical Chemistry, Am Faßberg 11, 37077 Göttingen, Germany.

[‡]Institute for Physical Chemistry, Georg-August University of Goettingen, Tammannstraße 6, 37077 Göttingen, Germany.

[§]International Center for Advanced Studies of Energy Conversion, Georg-August University of Goettingen, Tammannstraße 6, 37077 Göttingen, Germany

Corresponding Author

*E-mail: quan.shuai@mpibpc.mpg.de; sven.kaufmann@mpibpc.mpg.de

[‖]Present address: Institute for Molecules and Materials, Radboud University, Heijendaalseweg 135, Nijmegen 6525 AJ, the Netherlands.

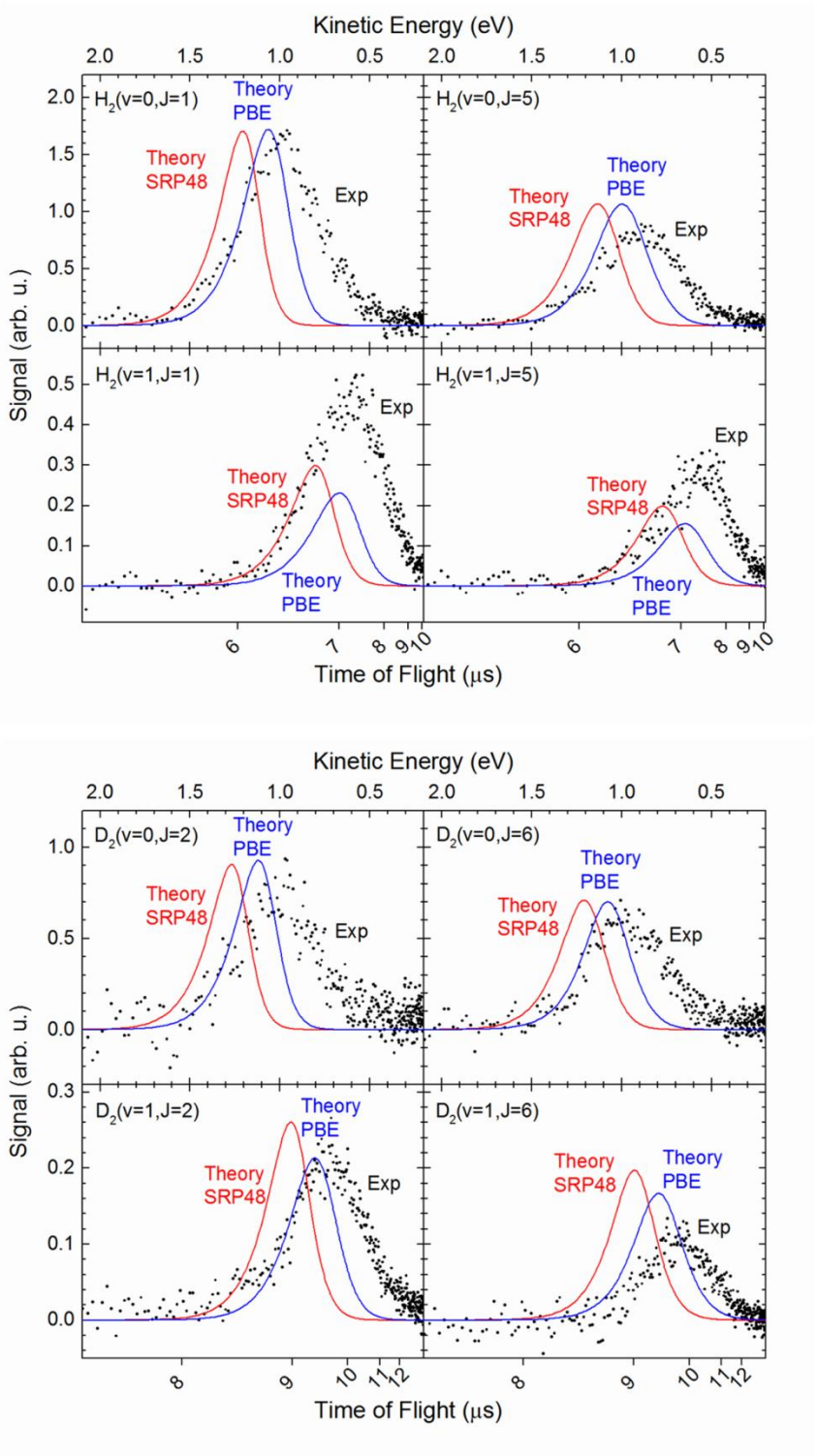

Figure S1. Experimental (black symbols) and theoretically predicted (red and blue lines) time-of-flight (TOF) distributions of H_2 and D_2 formed in associative desorption on Au(111).

Gaussian Parameters Describing the Measured Kinetic Energy Distributions of H_2 and D_2 Formed in Associative Desorption on Au(111)

To report the obtained experimental data independent of the detailed balance analysis, we also give Gaussian function parameters in tables S1-S4. These describe the flux in kinetic energy, which were obtained using equation S1:

$$f(E_{kin}, \mu, \sigma) = \frac{A(v,J)}{\sqrt{2\sigma^2\pi}} e^{\frac{-(E_{kin}-\mu)^2}{2\sigma^2}} . \quad \text{(S1)}$$

Here, the parameters are: $A(v,J)$, the amplitude of the peak, μ, the center and σ, the standard deviation. The experimental data was converted to flux in the kinetic energy scale and re-binned into bins of 40 meV. The fitting procedure excluded the thermal background by restricting to kinetic energies above 0.25 eV for v=0 and 0.15 eV for v=1, respectively. The algorithm used was the "lmfit"[1] module in python. The surface temperature was 1059-1063 K.

Tables S1-S4 give the resulting parameters together with their standard deviations (1σ, denoted by Δ) and the obtained reduced chi-square value of the fits. We point out that the amplitude parameters are only giving a relative scale.

J	$\boldsymbol{\mu}$ / eV	$\Delta\boldsymbol{\mu}$ / eV	$\boldsymbol{\sigma}$ / eV	$\Delta\boldsymbol{\sigma}$ / eV	$\boldsymbol{A}$ / arb. u.	$\Delta\boldsymbol{A}$ / arb. u.	χ_r^2
0	0.921	0.028	0.302	0.028	0.062	0.005	0.0136
1	0.938	0.009	0.234	0.009	0.509	0.017	0.0020
2	0.948	0.013	0.240	0.013	0.174	0.008	0.0453
3	0.917	0.010	0.221	0.010	0.332	0.012	0.1112
4	0.896	0.011	0.203	0.011	0.110	0.005	0.0205
5	0.840	0.007	0.243	0.007	0.251	0.007	0.0270
6	0.806	0.010	0.205	0.010	0.110	0.005	0.0151
7	0.747	0.008	0.216	0.008	0.125	0.004	0.0113
8	0.654	0.013	0.222	0.013	0.030	0.002	0.1546
9	0.643	0.008	0.219	0.009	0.043	0.002	0.0014

Table S1. Gaussian parameters describing the measured flux in kinetic energy scale for $H_2(v=0)$/Au(111)

J	$\boldsymbol{\mu}$ / eV	$\Delta\boldsymbol{\mu}$ / eV	$\boldsymbol{\sigma}$ / eV	$\Delta\boldsymbol{\sigma}$ / eV	$\boldsymbol{A}$ / arb. u.	$\Delta\boldsymbol{A}$ / arb. u.	χ_r^2
0	0.565	0.011	0.211	0.011	0.014	0.001	0.0003
1	0.563	0.006	0.219	0.006	0.112	0.003	0.0043
2	0.565	0.006	0.194	0.007	0.048	0.002	0.0015
3	0.563	0.005	0.204	0.005	0.137	0.003	0.0001
4	0.542	0.006	0.199	0.006	0.025	0.001	0.0003
5	0.529	0.005	0.196	0.006	0.060	0.002	0.0016
6	0.510	0.007	0.194	0.008	0.011	0.001	0.0001
7	0.490	0.007	0.199	0.007	0.022	0.001	0.0003

Table S2. Gaussian parameters describing the measured flux in kinetic energy scale for $H_2(v=1)$/Au(111)

J	$\boldsymbol{\mu}$ / eV	$\Delta\boldsymbol{\mu}$ / eV	$\boldsymbol{\sigma}$ / eV	$\Delta\boldsymbol{\sigma}$ / eV	$\boldsymbol{A}$ / arb. u.	$\Delta\boldsymbol{A}$ / arb. u.	χ_r^2
0	0.965	0.018	0.233	0.018	2.307	0.154	0.1764
1	0.976	0.013	0.215	0.013	1.378	0.072	0.0416
2	0.945	0.015	0.249	0.015	2.793	0.140	0.1351
3	0.935	0.013	0.240	0.013	1.216	0.057	0.0231
4	0.918	0.009	0.215	0.009	1.087	0.037	0.0105
5	0.922	0.019	0.252	0.019	0.577	0.038	0.9447
6	0.939	0.009	0.228	0.009	0.985	0.031	0.0072
7	0.917	0.012	0.184	0.012	0.308	0.017	0.2698
8	0.867	0.012	0.230	0.012	0.417	0.019	0.2549
9	0.856	0.016	0.270	0.016	0.212	0.011	0.0702
10	0.785	0.011	0.200	0.011	0.185	0.009	0.0646
12	0.694	0.009	0.199	0.009	0.166	0.006	0.0307

Table S3. Gaussian parameters describing the measured flux in kinetic energy scale for $D_2(v=0)$/Au(111)

J	$\boldsymbol{\mu}$ / eV	$\Delta\boldsymbol{\mu}$ / eV	$\boldsymbol{\sigma}$ / eV	$\Delta\boldsymbol{\sigma}$ / eV	$\boldsymbol{A}$ / arb. u.	$\Delta\boldsymbol{A}$ / arb. u.	χ_r^2
0	0.694	0.011	0.206	0.011	0.020	0.001	0.0008
1	0.681	0.008	0.202	0.008	0.029	0.001	0.0008
2	0.692	0.006	0.217	0.006	0.087	0.002	0.0027
3	0.681	0.008	0.208	0.008	0.037	0.002	0.0013
4	0.679	0.006	0.221	0.006	0.082	0.002	0.0030
5	0.668	0.008	0.187	0.008	0.034	0.002	0.0015
6	0.646	0.005	0.193	0.005	0.039	0.001	0.0007
7	0.628	0.009	0.204	0.009	0.024	0.001	0.0007
8	0.625	0.010	0.194	0.010	0.021	0.001	0.0007
9	0.616	0.017	0.232	0.017	0.013	0.001	0.0512

Table S4. Gaussian parameters describing the measured flux in kinetic energy scale for $D_2(v=1)$/Au(111)

Error Function Parameters Describing the Measured TOF Distributions of H_2 and D_2 Formed in Associative Desorption on Au(111)

The obtained TOF distributions were analyzed in terms of detailed balance, see eq. (1) in the main manuscript. The quantum state specific adsorption probability function contained in eq. (1), $S_0(E_{kin}, v, J)$, has been approximated with the error function:

$$S_0(E_{kin}, v, J) = A(v,J) \cdot \left[1 + \mathrm{erf}\left(\frac{E_{kin} - E_0(v,J)}{W(v)}\right)\right]. \quad \text{(S2)}$$

Here, the parameters are: $A(v,J)$, the saturation value, $E_0(v,J)$, the point of inflection of the curve and $W(v)$, the width of the curve. Due to poor signal to noise ratio for some of the obtained data, we found strong parameter variation and uncertainties when fitting those individually. This was circumvented by restricting $W(v)$ as a global parameter for data in the same vibrational state, irrespective of isotope and rotational state. This resulted in an increase of the overall fit reliability while not degrading the quality notably. Table S5 presents the $W(v)$ parameters as well as the obtained reduced chi-square value of these fits. The remaining fitted parameters are presented in tables S6 and S7. We note that the $A(v,J)$-parameters are on a relative scale and can only be compared for each isotope individually. Again, the algorithm used was the "lmfit"[1] module in python and the surface temperature was 1059-1063 K.

-	W / eV	ΔW / eV	χ_r^2
v=0	0.31	0.01	0.004295
v=1	0.29	0.01	0.002071

Table S5. Error function parameters obtained from detailed balance analysis, obtained from fitting the TOF distributions for both H_2 and D_2 from Au(111).

-	H_2 (v=0)			H_2 (v=1)		
J	E_0 / eV	ΔE_0 / eV	A / arb. u.	E_0 / eV	ΔE_0 / eV	A / arb. u.
0	1.31	0.02	0.6758	0.82	0.02	1.1711
1	1.31	0.01	0.9206	0.82	0.01	1.2185
2	1.32	0.01	0.8994	0.82	0.01	1.4028
3	1.29	0.01	0.5033	0.81	0.01	1.4576
4	1.26	0.01	0.6258	0.79	0.01	0.9338
5	1.21	0.01	0.4729	0.77	0.01	1.1475
6	1.17	0.01	1.0000	0.75	0.02	1.0816
7	1.10	0.01	0.5088	0.72	0.01	1.3291
8	1.00	0.03	0.3984	-	-	-
9	0.99	0.02	0.5491	-	-	-

Table S6. Error function parameters describing the measured TOF distribution for H_2/Au(111).

-	D_2 (v=0)			D_2 (v=1)		
J	E_0 / eV	ΔE_0 / eV	A / arb. u.	E_0 / eV	ΔE_0 / eV	A / arb. u.
0	1.36	0.03	1.0000	0.98	0.02	0.5562
1	1.36	0.03	0.8358	0.97	0.02	0.5220
2	1.33	0.01	0.6286	0.98	0.01	0.6070
3	1.32	0.02	0.5644	0.97	0.01	0.4252
4	1.29	0.02	0.2815	0.97	0.01	0.5006
5	1.30	0.02	0.4361	0.95	0.01	0.4695
6	1.32	0.02	0.7077	0.92	0.01	0.2911
7	1.28	0.03	0.6019	0.91	0.02	0.4443
8	1.24	0.02	0.4304	0.90	0.02	0.3031
9	1.23	0.04	0.7086	0.90	0.03	0.5811
10	1.14	0.03	0.3437	-	-	-
12	1.04	0.04	0.5670	-	-	-

Table S7. Error function parameters describing the measured TOF distribution for D_2/Au(111).

(1) Newville, M.; Stensitzki, T.; Allen, D. B.; Ingargiola, A. LMFIT: Non-linear least-square minimization and curve-fitting for Python, 2014.